Hyperspectral imagery denoising via reweighed sparse low-rank nonnegative tensor factorization

Fengchao Xiong[1] Jun Zhou[2] Yuntao Qian[1]

[1] College of Computer Science, Zhejiang University, Hangzhou, China
[2] School of Information and Communication Technology, Griffith University, Nathan, Australia

Introduction

In this paper, a reweighed sparse low-rank nonnegative tensor factorization (RSLRNTF) method is proposed to restore an HSI. It takes an HSI as a third-order tensor and factorizes it into the combination of a few component tensors where each one is the outer product of a low-rank matrix (coding matrix) and a vector (atom). A reweighed L_1 norm is added to coding matrices to enforce their sparsity. The low-rankness in both spatial and spectral domain is in line with the spatial and spectral correlation in an HSI. Furthermore, we add nonnegativity constraint to both coding coefficients matrices and dictionary to learn parts-based representation of HSI, which facilitates preserving local structure information.

RSLRNTF

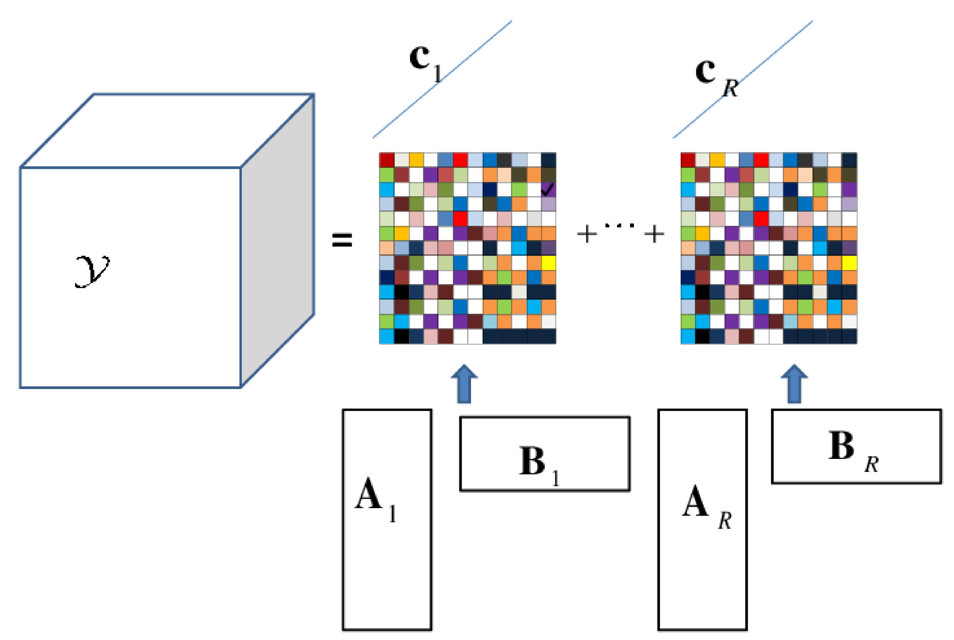

Figure 1: Framework of proposed method.

$$\min f(\mathbf{A},\mathbf{B},\mathbf{C}) = \|\mathcal{Y} - \sum_{r=1}^{R} \mathbf{A}_r\mathbf{B}_r^{\mathrm{T}} \circ \mathbf{c}_r\|_F^2 + \frac{\delta}{2}\|\mathbf{A}\mathbf{B}^{\mathrm{T}} - \mathbf{1}_{\mathbf{I}\times\mathbf{J}}\|_F^2 + \lambda\sum_{r=1}^{R}\|\mathbf{W}_r \odot (\mathbf{A}_r\mathbf{B}_r^{\mathrm{T}})\|_1 \quad s.t. \quad \mathbf{A}, \quad \mathbf{B}, \quad \mathbf{C} \geq 0$$

where, $\mathbf{A} = [\mathbf{A}_1 \cdots \mathbf{A}_R]$, $\mathbf{B} = [\mathbf{B}_1 \cdots \mathbf{B}_R]$, $\mathbf{C} = [\mathbf{c}_1 \cdots \mathbf{c}_R]$ and $\odot$ is element-wise product.

Highlights

- $\mathbf{A}_r\mathbf{B}_r^{\mathrm{T}}$: low-rank coding matrix derives spatial low-rankness.
- $\mathbf{C}$: low-rank dictionary represents spectral low-rankness.
- $\|\mathbf{W}_r \odot (\mathbf{A}_r\mathbf{B}_r^{\mathrm{T}})\|_1$: reweighed L_1 norm makes coding matrix sparser.
- $\frac{\delta}{2}\|\mathbf{A}\mathbf{B}^{\mathrm{T}} - \mathbf{1}_{\mathbf{I}\times\mathbf{J}}\|_F^2$: avoid trivial solutions.
- Nonnegativity constraints promote local details preserving.
- Tensor model preserves all the information in an HSI.

Update rules

$$\mathbf{A} \leftarrow \mathbf{A}.*(\mathbf{Y}_{(1)}^{\mathrm{T}}\mathbf{M} + \delta\mathbf{1}_{\mathbf{I}\times\mathbf{J}}\mathbf{B} + \mu\mathbf{U})./(\mathbf{A}\mathbf{M}^{\mathrm{T}}\mathbf{M} + \delta\mathbf{A}\mathbf{B}^{\mathrm{T}}\mathbf{B} + \mu\mathbf{A})$$
$$\mathbf{B} \leftarrow \mathbf{B}.*(\mathbf{Y}_{(2)}^{\mathrm{T}}\mathbf{M} + \delta\mathbf{1}_{\mathbf{I}\times\mathbf{J}}{}^{\mathrm{T}}\mathbf{A} + \mu\mathbf{V})./(\mathbf{B}\mathbf{M}^{\mathrm{T}}\mathbf{M} + \delta\mathbf{B}\mathbf{A}^{\mathrm{T}}\mathbf{A} + \mu\mathbf{B})$$
$$\mathbf{C} \leftarrow \mathbf{C}.*(\mathbf{Y}_{(3)}^{\mathrm{T}}\mathbf{M})./(\mathbf{C}\mathbf{M}^{\mathrm{T}}\mathbf{M})$$
$$\mathbf{U}_r \leftarrow \mathbf{U}_r.*(\mu\mathbf{A}_r)./(\mu\mathbf{U}_r + \lambda\mathbf{W}_r\mathbf{V}_r)$$
$$\mathbf{V}_r \leftarrow \mathbf{V}_r.*(\mu\mathbf{B}_r)./(\lambda\mathbf{W}_r^{\mathrm{T}}\mathbf{U}_r + \mu\mathbf{V}_r)$$
$$\mathbf{W}_r \leftarrow 1./(\mathbf{U}_r\mathbf{V}_r^{\mathrm{T}} + \epsilon)$$

Experimental results on simulated data

Table 1: MPSNR of Different Methods on Simulated Data.

Noise variance	$\sigma \in$[0, 0.05]	$\sigma \in$[0, 0.1]	$\sigma \in$[0, 0.15]
Original	34.49	26.89	24.84
LRMR [1]	43.12	39.12	36.63
LRTV [2]	43.04	37.63	36.26
PARAFAC [3]	38.58	37.51	35.99
TDL [4]	38.99	36.61	31.75
LRTDTV [5]	42.63	39.14	36.94
RSLRNTF	43.87	40.01	37.21

Visual comparison on simulated data

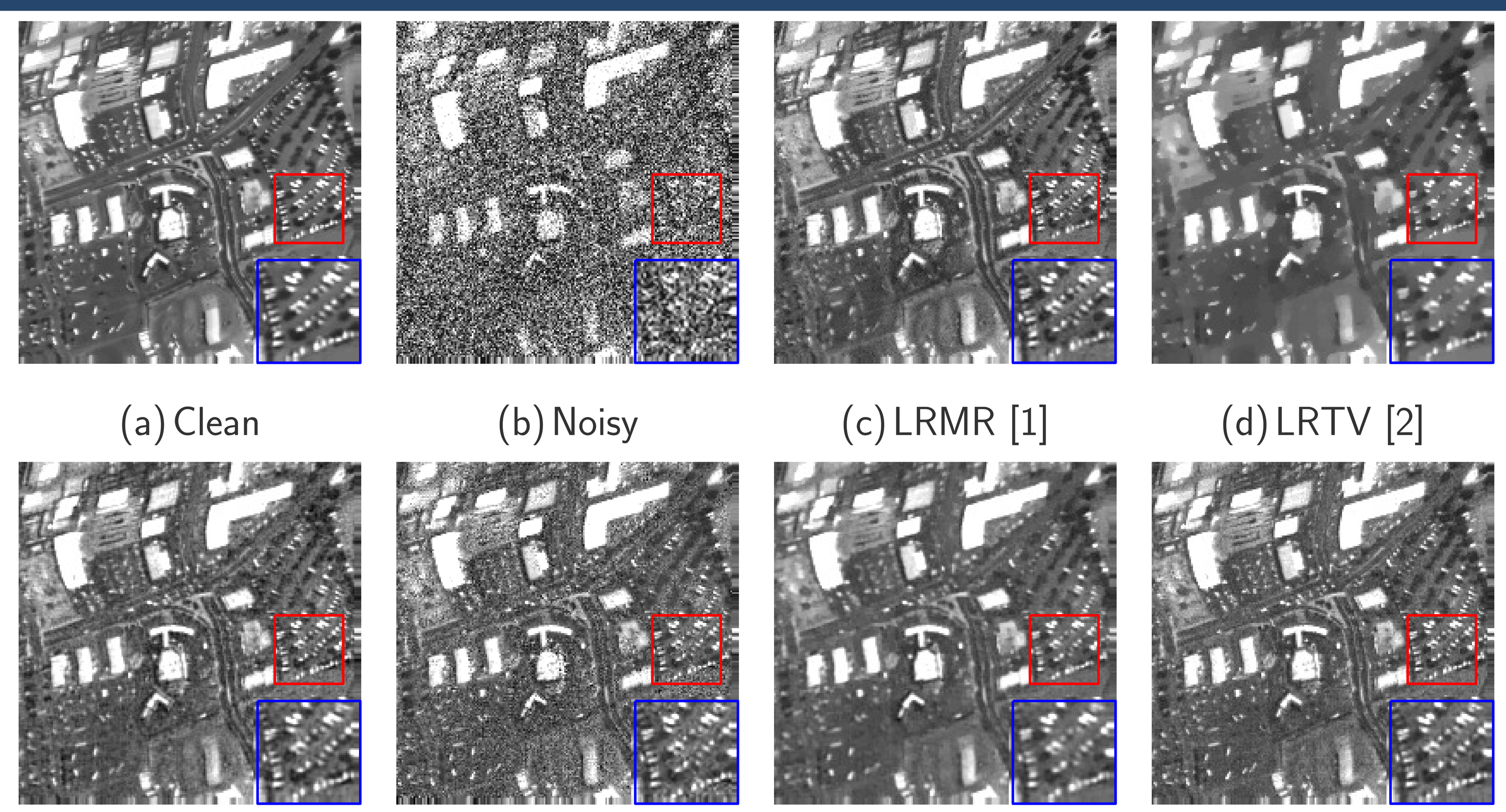

(a) Clean (b) Noisy (c) LRMR [1] (d) LRTV [2]
(e) PARAFAC [3] (f) TDL [4] (g) LRTDTV [5] (h) RSLRNTF

Figure 2: Denoising results of band 25 in simulated data when $\sigma \in [0 - 0.1]$.

Experimental results on real-world data

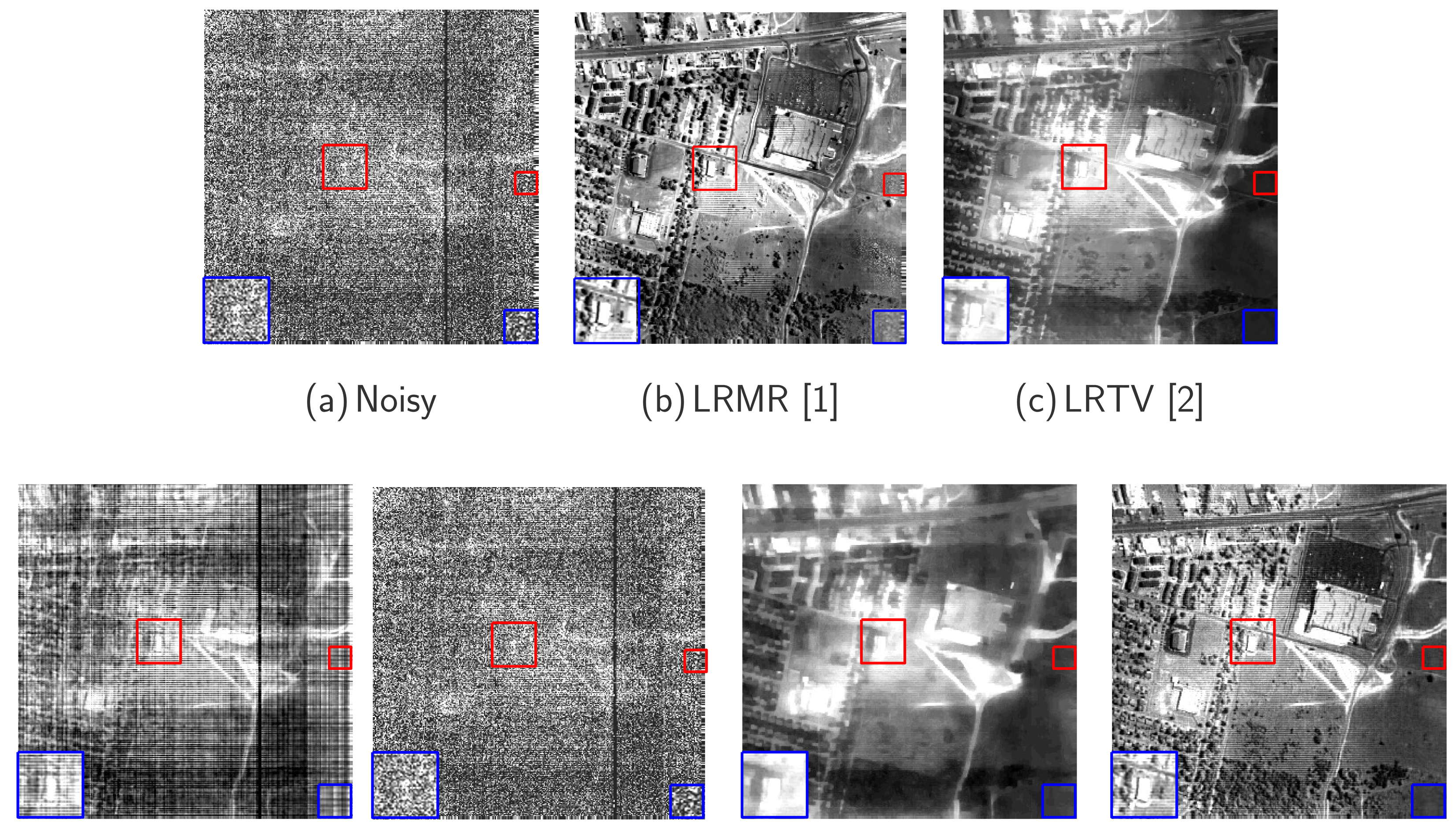

(a) Noisy (b) LRMR [1] (c) LRTV [2]
(d) PARAFAC [3] (e) TDL [4] (f) LRTDTV [5] (g) RSLRNTF

Figure 3: Denoising results of band 208 in the Urban data set.

References

[1] H. Zhang, W. He, L. Zhang, H. Shen, and Q. Yuan, "Hyperspectral image restoration using low-rank matrix recovery," *IEEE Trans. Geosci. Remote Sens.*, vol. 52, no. 8, pp. 4729–4743, Aug. 2014.

[2] W. He, H. Zhang, L. Zhang, and H. Shen, "Total-variation-regularized low-rank matrix factorization for hyperspectral image restoration," *IEEE Trans. Geosci. Remote Sens.*, vol. 54, no. 1, pp. 178–188, Jan. 2016.

[3] X. Liu, S. Bourennane, and C. Fossati, "Denoising of hyperspectral images using the parafac model and statistical performance analysis," *IEEE Trans. Geosci. Remote Sens.*, vol. 50, no. 10, pp. 3717–3724, Oct. 2012.

[4] Y. Peng, D. Meng, Z. Xu, C. Gao, Y. Yang, and B. Zhang, "Decomposable nonlocal tensor dictionary learning for multispectral image denoising," in *Proc. IEEE Conf. Comput. Vis. Patt. Recogn. (CVPR)*, Jun. 2014.

[5] Y. Wang, J. Peng, Q. Zhao, Y. Leung, X. Zhao, and D. Meng, "Hyperspectral image restoration via total variation regularized low-rank tensor decomposition," *IEEE J. Sel. Topics Appl. Earth Observ. Remote Sens.*, vol. 11, no. 4, pp. 1227–1243, 2018.